Int J Clin Exp Pathol 2024;17(9):268-286
www.ijcep.com /ISSN:1936-2625/IJCEP0157592

Original Article

Correlation of LOXL2 expression in non-small cell lung cancer with immunotherapy

Haoyan Chen*, Lele Liu*, Mingjiong Zhang, Shuangshuang Wu, Jianqing Wu

*Department of Geriatrics, Key Laboratory of Geriatrics of Jiangsu Province, The First Affiliated Hospital of Nanjing Medical University, 300 Guangzhou Road, Nanjing 210029, Jiangsu, China. *Equal contributors.*

Received May 6, 2024; Accepted August 25, 2024; Epub September 15, 2024; Published September 30, 2024

Abstract: Lung cancer is the most prevalent and lethal disease globally, with approximately 80% of cases being non-small cell lung cancer (NSCLC). NSCLC is primarily composed of lung squamous cell carcinoma (LUSC) and lung adenocarcinoma (LUAD). Despite chemotherapy currently being the primary treatment for NSCLC, chemotherapy resistance remains a significant challenge for patients. Recent studies have proposed immunotherapy as a promising new avenue for treating NSCLC. The association between the lysyl oxidase-like 2 (LOXL2) gene and NSCLC was explored using multiple online tools and bioinformatics analysis software based on the available datasets from TCGA. The immune microenvironment of the tumor was explored by calculating ImmuneScore, StromalScore, and TumorPurity of LUAD and LUSC and analyzing the infiltration of 22 immune cells in lung cancer tissues. LOXL2-related loads were obtained from the Xena database for LUSC and LUAD patients, and relevant prognostic genes were identified by analyzing survival curves. Functional and pathway enrichment analyses of prognostic, predictive genes were performed using Gene Ontology (GO) and the Kyoto Encyclopedia of Genes and Genomes (KEGG). The expression of LOXL2 in NSCLC was detected by RT-qPCR. LOXL2 may be involved in the progression of LUAD and LUSC and is closely related to the T-lymphocyte subpopulation, T-reg cells. SEMA7A and VEGFC are identified as the genes that interact with LOXL2 and could be used as prognostic signature genes in NSCLC patients. LOXL2 may become a prognostic marker and a new target for immunotherapy.

Keywords: NSCLC, bioinformatics, immune infiltration, *LOXL2*, doxorubicin

Introduction

Lung cancer stands as a leading cause of cancer-related mortality worldwide, contributing to an estimated 26% of global cancer-related fatalities [1-3]. Amongst all lung cancer cases, non-small cell lung cancer (NSCLC) accounts for roughly 80%, further classify into lung squamous cell carcinoma (LUSC) and lung adenocarcinoma (LUAD) [4, 5]. Decades of intensive genomic and signaling pathway research have revealed that NSCLC constitutes a diverse group of diseases characterized by genetic and cellular heterogeneity [6], primarily encompassing LUSC and LUAD [7]. Notably, early-stage NSCLC often exhibits mild symptoms and clinical signs, posing challenges for early detection. The aggressive nature and rapid progression of NSCLC frequently lead to patients presenting with locally advanced or metastatic disease at diagnosis [8].

Surgical resection is the preferred therapeutic modality for patients diagnosed with early-stage NSCLC, whereas a multimodal approach combining radiotherapy and chemotherapy is typically employed for those presenting with advanced, inoperable disease stages [9]. However, resistance to chemotherapeutic agents such as cisplatin has been a significant challenge, necessitating the development of new approaches to treat NSCLC [10]. In recent years, there has been growing recognition of the benefits of harnessing the host's immune system to combat malignancy [11, 12]. The emergence of immunotherapy has revolutionized the landscape of NSCLC treatment by capitalizing on this concept [13]. The underlying principle of immunotherapy involves the stimulation of the patient's endogenous T-cells and the subsequent release of cytokines, which facilitate the targeted destruction of tumor cells [14]. At present, the principal immune

https://doi.org/10.62347/ZIEG9007

checkpoints are PD-1 and PD-2 [15]. Prior investigations have demonstrated the promise of neoadjuvant immunotherapy in patients with substantial tumor burden [16]. Furthermore, an intricate interplay between regulatory T-cells (Tregs) and the tumor microenvironment has been well-documented in numerous studies, underscoring the importance of further exploration into novel targets for immunotherapy [17]. It is therefore of interest to explore new targets for the immunotherapy of NSCLC. The expression of *LOXL2* is markedly elevated in tumors, contributing to tumor invasion and migration [18]. However, the utility of *LOXL2* as a target for immunotherapy in NSCLC remains uncharted territory and merits further investigation.

In this study, we conducted a bioinformatics analysis of the risk factors influencing the prognosis of non-small cell lung cancer (NSCLC) using differential gene expression, survival curves, the tumor immune microenvironment, associations with other molecules, and KEGG and GO analysis. Furthermore, RT-qPCR analysis demonstrated that LOXL2 was highly expressed in NSCLC. The aforementioned results indicate that LOXL2 may serve as a promising target for immunotherapy in NSCLC patients.

Material and methods

Gene expression data analysis

Inclusion criteria for this study were as follows: (a) pathologic diagnosis of NSCLC (biopsy or surgically resected tissue), (b) no experience of immunotherapy and other radiotherapy, and (c) having complete gene sequencing results. The exclusion criteria were as follows: (a) incomplete information; (b) combination with other tumors. In the TCGA database, GEPIA identifies the top 500 differentially expressed genes (DEGs) in LUAD and LUSC patients, and subsequently identified 11 commonly related genes by intersecting the results. Subsequently, Kaplan-Meier plotter 2 was employed to assess the overall survival (OS) of LUAD and LUSC cancer patients. The samples were divided into two groups according to gene expression levels in order to determine the significance of each gene in predicting the patient's prognosis. Subsequently, a Kaplan-Meier survival curve was constructed to compare the two groups and contrast the log10HR value (HRs) and *P*-value. The two risk factors, LOXL2 and TLDC1, with the most unfavorable prognosis in LUAD and LUSC, were identified. A total of 483 cases of lung adenocarcinoma (LUAD) and 486 cases of lung squamous cell carcinoma (LUSC) were included in the analysis from the GEPIA database. The cases were designated as the "tumor group", and the expression of LOXL2 in this group was compared with that of the "control group".

Tumor purity and immune cell infiltration analysis

The ESTIMATE algorithm was employed to calculate ImmuneScore, StromalScore, and Tumor Purity for LUAD and LUSC patients, respectively. The proportion of 22 TILs in LUSC and LUAD was determined using the R package CIBERSORT. Furthermore, GEPIA2021 was employed to visualize gene expression profiles in order to explore the differences in immune cell subtypes. The immune cells included in this study were neutrophils, eosinophils, mast cells, and mast cells in different states of activation. The following cell types were identified: dendritic cells activated, dendritic cells quiescent, macrophages M2, T cell follicular helper cells, T cell regulatory (Tregs), T cell γδ, NK cells quiescent, NK cells activated, monocytes, macrophages M0, macrophages M1, T cell CD4 memory activated, T cell CD4 memory quiescent, T cell CD4 naive, T cell CD8, plasma cells, B cell memory, and B cell naive.

Immune prognosis analysis of LOXL2

ssGSEA was used to analyze the immune profile of *LOXL2* in LUAD and LUSC, and the tumor tissues of LUAD and LUSC in the GEPIA database were compared to the adjacent tissues in normal lungs. The results demonstrated a significant positive correlation between LUAD and T-reg (rho=0.311, P=5.71e-13) and between LUSC and T-reg (rho=0.494, P<2.2e-16).

Correlated gene analysis

LOXL2-associated genes from LUAD and LUSC patients were obtained using the Xena database, *P*-values and *R*-values were calculated, and differentially expressed genes (DEGs) were analyzed. Cross-tabulation analysis was performed on genes that were upregulated in

Table 1. List of primers

Gene	Primer (5'-3')
LOXL2	F: AACGAGGCGACCCTTGCAGC
	R: GGGTGCGCTTGCGGTAGGTT
GAPDH	F: CTCCTCCACCTTTGACGC
	R: CCACCACCCTGTTGCTGT

LOXL2-associated genes in LUAD and LUSC patients. The eight cross-over genes associated with OS were extracted by univariate Cox regression analysis of the results and then the median of their characteristic scores. Patients were finally categorized as high and low risk. Patient survival was analyzed by the Kaplan-Meier method. Time-dependent receiver operating characteristic (ROC) curves were used to predict the accuracy and characteristics of clinical characteristics. The R package rms was employed to generate the nomograms.

Genetic interaction analysis

The search tool for interacting genes/proteins (STRING) database (http://cn.string-bd.org) was used to establish a PPI network of *LOXL2*.

Gene enrichment analysis

GO and KEGG analysis was carried out by using the R package "clusterProfiler". Gene Ontology (GO) was used for functional enrichment analysis, while the Kyoto Encyclopedia of Genes and Genomes (KEGG) was used for pathway enrichment analysis. The effects of functional enrichment included molecular functions (MF), cellular components (CC), and biological processes (BP). The top 10 pathway enrichment was analyzed.

Drug sensitivity analysis

We used the "oncoPredict" R package to analyze the batch-corrected prioritization of different drugs in the DREAMT database.

Cell culture

Human bronchial epithelial cell line, human non-small cell lung cancer cell line PC9, A549, H1299 were provided by Jiangsu Province Key Laboratory of Geriatrics, and cultured in DMEM (Sigma-Aldrich) supplemented with 100 μg/ml streptomycin, 100 μg/ml penicillin (Gibco), and 10% fetal bovine serum (FBS) (Invitrogen). All cells were maintained in a 5% CO_2 incubator (Thermo Fisher Scientific) at 37°C. Cells in the logarithmic growth phase were used for experiments.

RT-PCR

Total RNA was extracted from the cells using Trizol reagent (Invitrogen). RNA was reverse transcribed to cDNA using Primescript™ RT Master Mix (Vazyme). Quantitative RT-PCR was performed using ChamQTM Universal SYBR QPCR Master Mix (Vazyme) and Steppe One PlusTM Real-Time PCR System (Application Biosystems, Foster City, CA, USA). The primers for *LOXL2* and *GAPDH* (used as an internal reference) were purchased from Genscript. RT-PCR was performed under the following conditions: Fluorescence signal was acquired at 94° for 60 seconds, 95° for 10 seconds and 60° for 30 seconds, and after 40 cycles, 60° were acquired. Target gene expression levels were normalized to GAPDH expression and then calculated using the $2^{-\Delta\Delta Ct}$ method. The primer sequences are listed in **Table 1**.

Cell viability

The Cell Counting Kit-8 (Vazyme) was performed to detect cell proliferation. We purchased doxorubicin from Beijing Huamei Company and used it to treat 1×10^4 cells in a 96-well plate. The cells were exposed to different concentrations of doxorubicin for 24 hours. 10 μl CCK8 reagent was added into each well according to the instruction of CCK8. Then, absorbance of samples was detected at 450 nm wavelength.

Statistical analysis

Kaplan-Meier plots used HR and *P*-value or Cox *P*-value for the log-rank test. Comparisons were made using unpaired and paired t-tests for normally distributed variables or Mann-Whitney U-test and Wilcoxon signed-rank test for non-normally distributed variables. R software was used to perform all statistical analyses. *P*-value <0.05 was considered significant.

Results

Expression feature of LOXL2

We identified the top 500 DEGs in LUAD and LUSC from the TCGA databases. We crossed

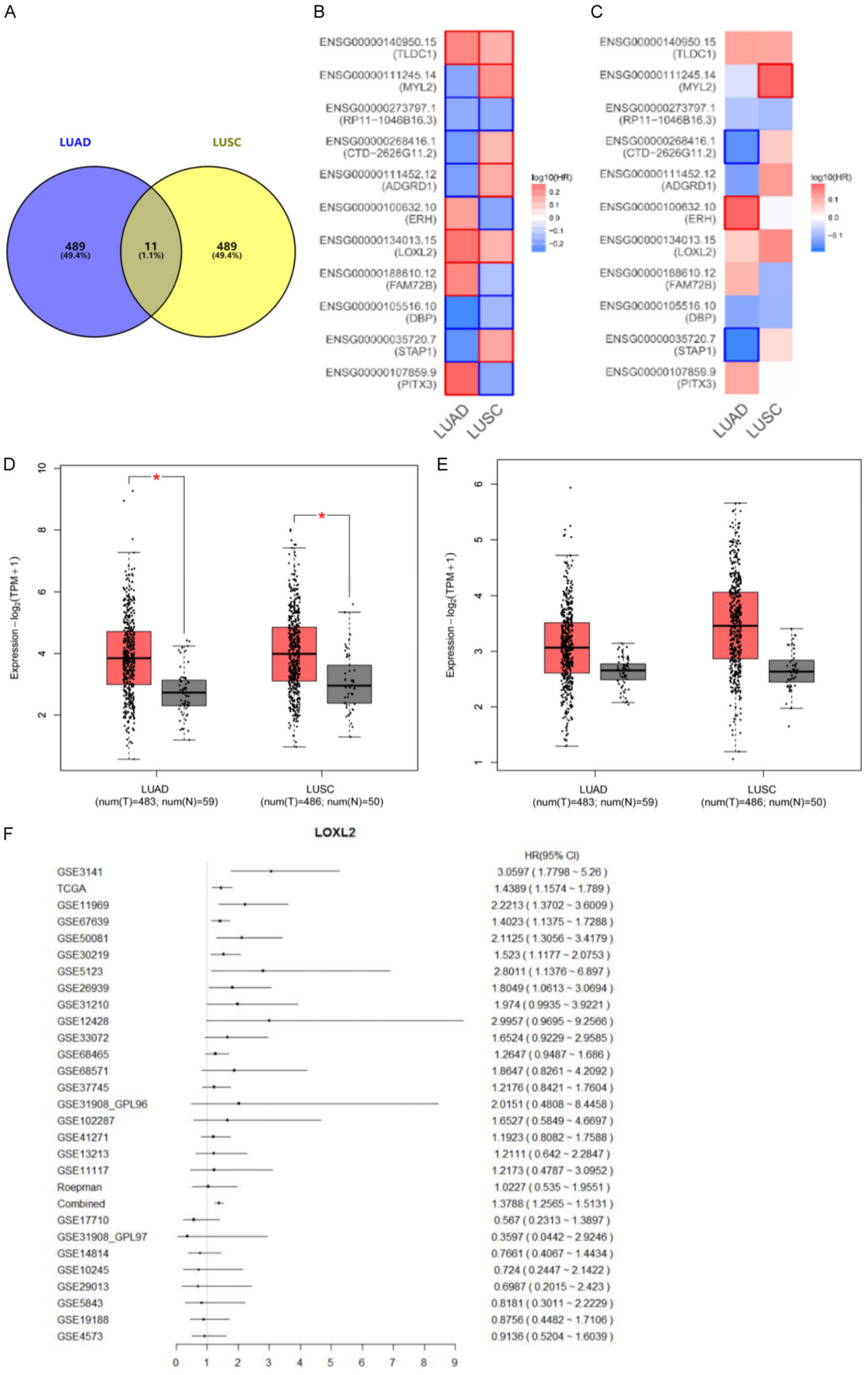
A
LUAD
LUSC
489
(49.4%)
11
(1.1%)
489
(49.4%)
B
ENSG00000140950.15
(TLDC1)
ENSG00000111245.14
(MYL2)
ENSG00000273797.1
(RP11−1046B16.3)
ENSG00000268416.1
(CTD−2626G11.2)
ENSG00000111452.12
(ADGRD1)
ENSG00000100632.10
(ERH)
ENSG00000134013.15
(LOXL2)
ENSG00000188610.12
(FAM72B)
ENSG00000105516.10
(DBP)
ENSG00000035720.7
(STAP1)
ENSG00000107859.9
(PITX3)
log10(HR)
LUAD
LUSC
C
log10(HR)
LUAD
LUSC
D
Expression − log2(TPM+1)
LUAD
(num(T)=483; num(N)=59)
LUSC
(num(T)=486; num(N)=50)
E
Expression − log2(TPM+1)
LUAD
(num(T)=483; num(N)=59)
LUSC
(num(T)=486; num(N)=50)
F
LOXL2
HR(95% CI)
GSE3141 3.0597 (1.7798 ~ 5.26)
TCGA 1.4389 (1.1574 ~ 1.789)
GSE11969 2.2213 (1.3702 ~ 3.6009)
GSE67639 1.4023 (1.1375 ~ 1.7288)
GSE50081 2.1125 (1.3056 ~ 3.4179)
GSE30219 1.523 (1.1177 ~ 2.0753)
GSE5123 2.8011 (1.1376 ~ 6.897)
GSE26939 1.8049 (1.0613 ~ 3.0694)
GSE31210 1.974 (0.9935 ~ 3.9221)
GSE12428 2.9957 (0.9695 ~ 9.2566)
GSE33072 1.6524 (0.9229 ~ 2.9585)
GSE68465 1.2647 (0.9487 ~ 1.686)
GSE68571 1.8647 (0.8261 ~ 4.2092)
GSE37745 1.2176 (0.8421 ~ 1.7604)
GSE31908_GPL96 2.0151 (0.4808 ~ 8.4458)
GSE102287 1.6527 (0.5849 ~ 4.6697)
GSE41271 1.1923 (0.8082 ~ 1.7588)
GSE13213 1.2111 (0.642 ~ 2.2847)
GSE11117 1.2173 (0.4787 ~ 3.0952)
Roepman 1.0227 (0.535 ~ 1.9551)
Combined 1.3788 (1.2565 ~ 1.5131)
GSE17710 0.567 (0.2313 ~ 1.3897)
GSE31908_GPL97 0.3597 (0.0442 ~ 2.9246)
GSE14814 0.7661 (0.4067 ~ 1.4434)
GSE10245 0.724 (0.2447 ~ 2.1422)
GSE29013 0.6987 (0.2015 ~ 2.423)
GSE5843 0.8181 (0.3011 ~ 2.2229)
GSE19188 0.8756 (0.4482 ~ 1.7106)
GSE4573 0.9136 (0.5204 ~ 1.6039)
0 1 2 3 4 5 6 7 8 9

Figure 1. *LOXL2* is highly expressed in non-small cell lung cancer. A. Venn diagrams of the top 500 abnormally expressed genes related to LUAD and LUSC (R package analysis). B. Survival analysis of 11 intersection gene expression levels in LUAD and LUSC. C. *LOXL2* and *TLDC1* are associated with shorter overall survival. D, E. The level of *LOXL2* in LUAD and LUAC cancer tissues is higher than in para cancer. F. Univariate analysis was used to analyze the correlation between LOXL2 expression and clinical prognosis in NSCLC patients.

them to obtain eleven common DEGs, including *PITX3, STAP1, DBP, FAM72B, LOXL2, ERH, ADGRD1, CTD-2626G11.2, RP11-1046B16.3, MYL2, TLDC1* (**Figure 1A**). Next, we used Kaplan-Meier Plotter and GEPIA database to explore the relationship between this set of genetic changes and the survival rate of LUAD and LUDSC patients (Figures S1, S2). We found six protective factors: *STAP1, DBP, ADGRD1, CTD-2626G11.2, 1046B16.3, MYL2* and five risk factors: *PITX3, FAM72B, LOXL2, ERH, TLDC1*. Among these, we focused on two risk factors *LOXL2* and *TLDC1*, which had high-risk values in LUAD and LUSC (**Figure 1B**, **1C**). Based on the GEPIA dataset, we analyzed *LOXL2* and *TLDC1* in lung cancer tissues and adjacent tissues. We included lung cancer cases (n=483 for LUAD; n=486 for LUSC) as the "tumor group". Compared to the "control group", we found that the expression level of *LOXL2* in the "tumor group" was higher (**Figure 1D**, **1E**).

Furthermore, we verified that *LOXL2* was highly expressed in LUAD and LUSC by calculating the *p*-value, HR value, and 95% cl of the *LOXL2* gene in the Oncomine database and TCGA database (P<0.05) (**Figure 1F**; **Table 2**).

LOXL2-related immune cell infiltration

We performed the immune score, stromal score, and tumor purity determinations of *LOXL2* (**Figure 2A-F**), and the results showed that *LOXL2* is negatively correlated with an immune score, positively correlated with a stromal score, and negatively associated with tumor purity. Considering that the tumor immune microenvironment plays a significant role in the development of tumorigenesis, we then used the R package CIBERSORT to determine the ratio of 22 TILs in LUAD and LUSC patients (**Figures 2G**, **2H**, S3A, S3B).

LOXL2 was positively correlated with T-reg

We characterized the immunology profile of LUAD and LUSC samples with low *LOXL2* and high *LOXL2* expression by ssGSEA. Found that *LOXL2* in LUAD and LUSC patients is associated with T-reg. GEPIA, to compare LUAD and LUSC tumor tissues, adjacent tissues, and normal lungs (**Figure 3A**, **3B**), found highly expressed T-reg in tumor tissues. In addition, Spearman Correlation Text confirmed the positive correlation between LUAD (**Figure 3C**) and LUSC (**Figure 3D**), and T-reg (LUAD, T-reg rho=0.311, P=5.71e-13; LUSC, T-reg, rho= 0.494, P<2.2e-16). All these results indicated that *LOXL2* might potentially regulate immune infiltration and the response to immunotherapy.

Correlated gene expression

Furthermore, we evaluated the association of fifty-two corresponding bases of LUAD (**Figure 4A**; **Table 3**) and ten related genes of LUSC (Figure S4; **Table 4**) with *LOXL2*. Based on the intersection of the related genes of LUAD and LUSC and *LOXL2*, we identified eight common genes (**Figure 4B**): *PDGFRA*, *SEMA7A*, *FGF5*, *CMTM3*, *UCN2*, *MANF*, *PDGFC*, *VEGFC*. Among them, *LOXL2, SEWA7A, FGF5, UCN2,* and *VEGFC* were positively correlated with LUAD; while *LOXL2, SEMA7A,* and *VEGFC* were positively correlated with LUSC (all P<0.05) (**Figure 4C**).

Predictive significance of SEMA7A and VEGFC in LUAD and LUSC

The common genes *SEMA7A* and *VEGFC* related to LUAD, LUSC, and *LOXL2* were used as independent factors for Cox survival analysis (**Figure 5A-D**). *SEMA7A* (Log-rank P=0.016) and *VEGFC* (Log-rank P<0.01) were prognostic factors in LUAD. *SEMA7A* (Log-rank P=0.0017) and *VEGFC* (Log-rank P=0.003) were predictive factors in LUSC.

Next, we built a PPI network to understand the mode of interaction of *LOXL2* (**Figure 5E**). The PPI network comprised 31 nodes, showing the relationship between *LOXL2*, *SEMA7A*, and *VEGFC*. The results prove that *SEMA7A* and *VEGFC* are prognostic factors of LUAD and LUSC.

Table 2. Univariate analysis of the correlation between LOXL2 expression and clinical features and OS in LUAD and LUSC patients

Dataset	*P* value	HR	95% CI	Prognostic	
GSE3141	<0.0001	3.0597	1.7798-5.2600	Poor	Go
TCGA	0.0011	1.4389	1.1574-1.7890	Poor	Go
GSE11969	0.0012	2.2213	1.3702-3.6009	Poor	Go
Stage I	0.1672	1.7682	0.7876-3.9693		
Stage II	0.516	1.5434	0.4166-5.7188		
Stage III	0.0014	3.4612	1.6128-7.4280	Poor	Go
GSE67639	0.0015	1.4023	1.1375-1.7288	Poor	Go
GSE50081	0.0023	2.1125	1.3056-3.4179	Poor	Go
Stage I	0.0428	1.8640	1.0203-3.4056	Poor	Go
Stage II	0.1498	1.7766	0.8127-3.8839		
GSE30219	0.0077	1.5230	1.1177-2.0753	Poor	Go
GSE5123	0.0251	2.8011	1.1376-6.8970	Poor	Go
Stage I	0.4481	1.7116	0.4269-6.8620		
Stage II	0.2313	2.4212	0.5692-10.3000		
Stage III	0.2918	3.6458	0.3290-40.3971		
GSE26939	0.0293	1.8049	1.0613-3.0694	Poor	Go
Stage I	0.1121	1.8641	0.8646-4.0194		
Stage III	0.1187	2.6001	0.7828-8.6362		
GSE31210	0.0522	1.9740	0.9935-3.9221		
Stage I	0.0015	4.7791	1.8171-12.5698	Poor	Go
Stage II	0.3536	0.5551	0.1601-1.9252		
GSE12428	0.0566	2.9957	0.9695-9.2566		Go
GSE33072	0.0910	1.6524	0.9229-2.9585		Go
GSE68465	0.1093	1.2647	0.9487-1.6860		Go
GSE68571	0.1336	1.8647	0.8261-4.2092		Go
Stage I	0.2186	1.9920	0.6646-5.9708		
Stage II	0.4599	0.5556	0.1169-2.6405		
GSE17710	0.2148	0.5670	0.2313-1.3897		Go
Stage I	0.6453	1.2765	0.4514-3.6101		
Stage II	0.0807	0.1560	0.0194-1.2551		
GSE37745	0.2954	1.2176	0.8421-1.7604		Go
Stage I	0.3817	1.2318	0.7721-1.9651		
GSE37745	0.2954	1.2175	0.8421-1.7604		Go
Stage I	0.3817	1.2176	0.7721-1.9651		
Stage II	0.2517	1.2318	0.7032-3.8342		
Stage III	0.0789	1.6420	0.1594-1.1054		
GSE31908_GPL96	0.3379	0.4198	0.4808-8.4458		Go
Stage I	0.4208	2.0151	0.1952-49.9487		
GSE31908_GPL97	0.3389	3.1225	0.0442-2.9246		Go
GSE102287	0.3431	0.3697	0.5849-4.6697		Go
GSE41271	0.3752	1.6527	0.8082-1.7588		Go
Stage I	0.0460	1.1923	1.0119-3.6844	Poor	
Stage II	0.2885	1.9308	0.1872-1.6460		
Stage III	0.5018	0.5550	0.4432-1.4893		
GSE14814	0.4097	0.8125	0.4067-1.4434		Go
Stage I	0.5010	0.7661	0.2710-1.8932		

Stage II	0.0585	0.7163	0.4185-2.0663		
GSE13213	0.5543	0.9299	0.6420-2.2847		Go
Stage III	0.1295	1.2111	0.7902-6.3195		
GSE10245	0.5596	2.2347	0.24472.1422		Go
GSE29013	0.5720	0.7240	0.2015-2.4230		Go
Stage I	0.8679	0.6987	0.0916-7.5108		
Stage III	0.7513	0.8295	0.1581-3.7854		
GSE11117	0.6797	0.7736	0.4787-3.0952		Go
Stage IV	0.7480	1.2173	0.3764-3.8970		
GSE5843	0.6938	1.2112	0.3011-2.2229		Go
Stage I	0.6080	0.8181	0.2301-2.0696		
GSE19188	0.6975	0.6901	0.4482-1.7106		Go
GSE4573	0.7531	0.8756	0.5204-1.6039		Go
Stage I	0.9703	1.0146	0.4719-2.1815		
Stage II	0.2390	1.8968	0.6522-5.5165		
Stage III	0.2249	0.4603	0.1315-1.6114		
Poepman	0.9458	1.0227	0.5350-1.9551		Go
combined	<0.0001	1.3787	1.2564-1.5130	Poor	

Note: cutoff: upper 25% VS other 75%.

Enrichment of LOXL2-correlated gene

GO enrichment analysis in terms of biological processes (BP), cellular components (CC) and molecular functions (MF) revealed that the significant regulatory processes of *LOXL2* on BP were axonogenesis, axon guidance, and neuronal projection guidance (**Figure 6A**). For CC, alterations in *LOXL2* most clearly controlled processes in the semaphorin receptor complex and the collagen-containing extracellular matrix (**Figure 6B**). In the results shown for MF, semaphorin receptor activity was the most responsive to regulation by *LOXL2*, which was most clearly associated with different sites of regulation (**Figure 6C**).

KEGG pathway enrichment of the *LOXL2* interactive gene showed that axon guidance, focal adhesion, and PI3K-Akt signaling pathway were enriched pathways (**Figure 6D**).

*Therapeutic targets and mechanisms of drug*s

Volcano plots showed the priorities of different drugs in the DREAMT database and after batch correction (**Figure 7A**). Then we analyzed the marketing status of all oncology drugs (**Figure 7B**). A large proportion of experimental drugs are approved, mainly including dopamine receptor antagonists, cyclooxygenase inhibitors, serotonin receptor antagonists, glucocorticoid receptor antagonists, adrenergic receptor agonist, adrenergic receptor antagonists, and bacterial cell wall synthesis inhibitor (**Figure 7C**). Further analyses screened nine drugs: cefuroxime benzocaine, benzocaine, cefazolin, methotrexate, tacrolimus, rimantadine, doxorubicin, cefuroxime, guanethidine (**Table 5**).

Drug sensitivity experiments of doxorubicin on LOXL2 expression profile

To further substantiate the predicted drug response to *LOXL2* inhibition, we selected doxorubicin, the agent displaying the strongest correlation with our target gene, for subsequent experimental validation. We initially assessed the expression levels of *LOXL2* across three commonly used non-small cell lung cancer (NSCLC) cell lines: PC9, A549, and H1299. These expression profiles were quantified via quantitative PCR (qPCR) analysis. As illustrated in the Figure, the H1299 cell line, exhibiting robust LOXL2 expression, and the PC9 cell line, characterized by relatively low *LOXL2* expression, were chosen for our drug sensitivity studies (**Figure 8A**). We then employed a Cell Counting Kit-8 (CCK-8) assay to determine the half-maximal inhibitory concentration (IC_{50}) of doxorubicin at various dose gradients in both the H1299 and PC9 cell lines (**Figure 8B**, **8C**). The IC_{50} of H1299 was determined to be 2.248 μg/ml. Furthermore, the IC_{50} of PC9 was 6.026

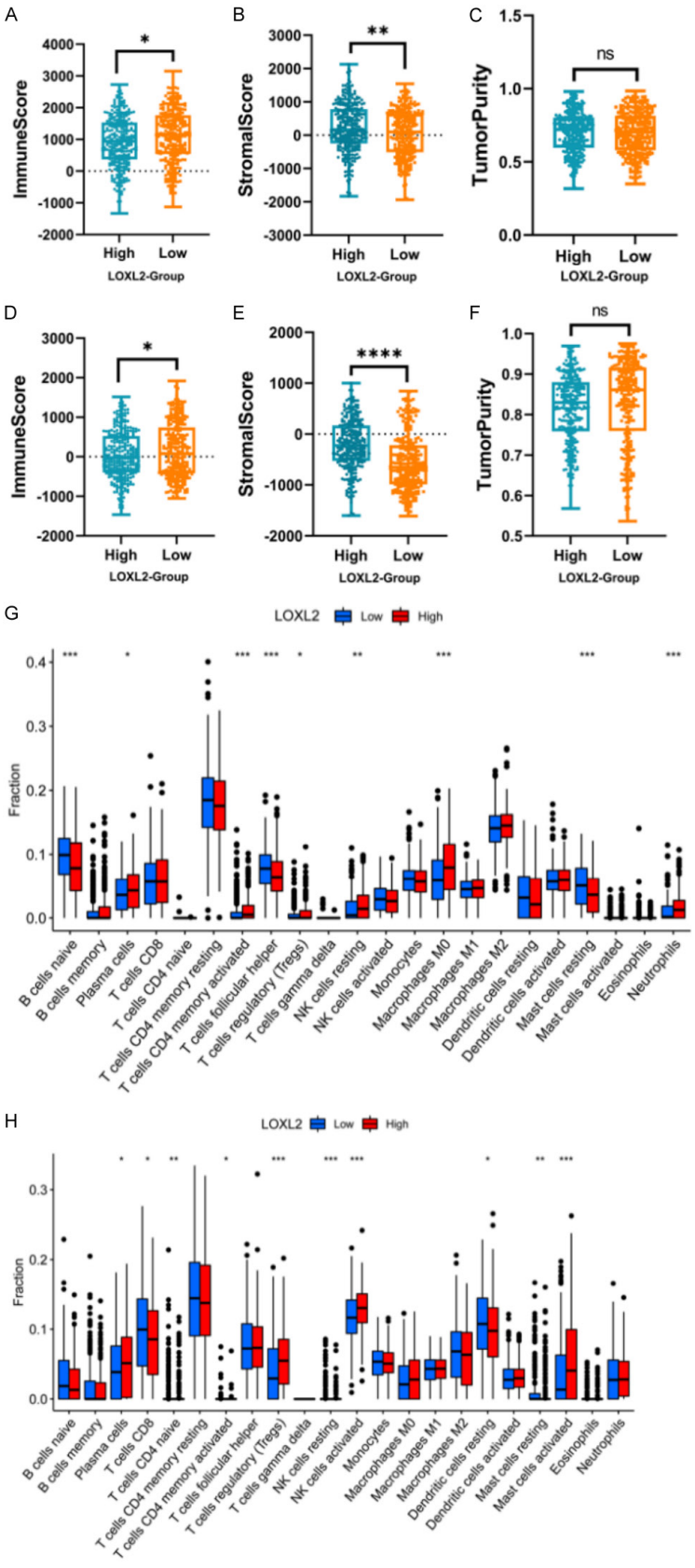

Figure 2. LOXL2 is associated with tumor microenvironment and tumor mutation burden. A-F. Use box plots to show the immune score, stromal score, and tumor purity of *LOXL2* on LUAD and LUSC. G, H. Taking the median TMB value as a cutoff, the relative expressions of 22 tumor-infiltrating immune cells in the low- and high-TMB samples were determined (P<0.05, P<0.01, P<0.001, ns, not significant).

μg/ml (P<0.05), indicating that the high *LOXL2*-expressing cell line H1299 exhibited greater sensitivity to doxorubicin than the low *LOXL2*-expressing cell line PC9.

Discussion

Many patients with non-small cell lung cancer are diagnosed at an advanced stage, and those diagnosed in an early stage often relapse and develop metastatic lesions, despite recent advances in treatment [19]. Tumor immunotherapy has developed rapidly and has attracted increasing attention due to its effectiveness [20-22]. In light of this, our study aims to discover new targets for immunotherapy and predictive indicators for NSCLC patients. We began by the intersecting 500 differentially expressed genes (DEGs) found in both lung adenocarcinoma (LUAD) and lung squamous cell carcinoma (LUSC), then perform survival curve analysis on the 11 genes shared between the two groups. Additionally, we compared the expression levels of these 11 genes in para-cancerous and lung cancerous tissues, ultimately identifying LOXL2 as a promising biomarker.

The lysyl oxidase (LOX) family, currently comprising LOXL1,

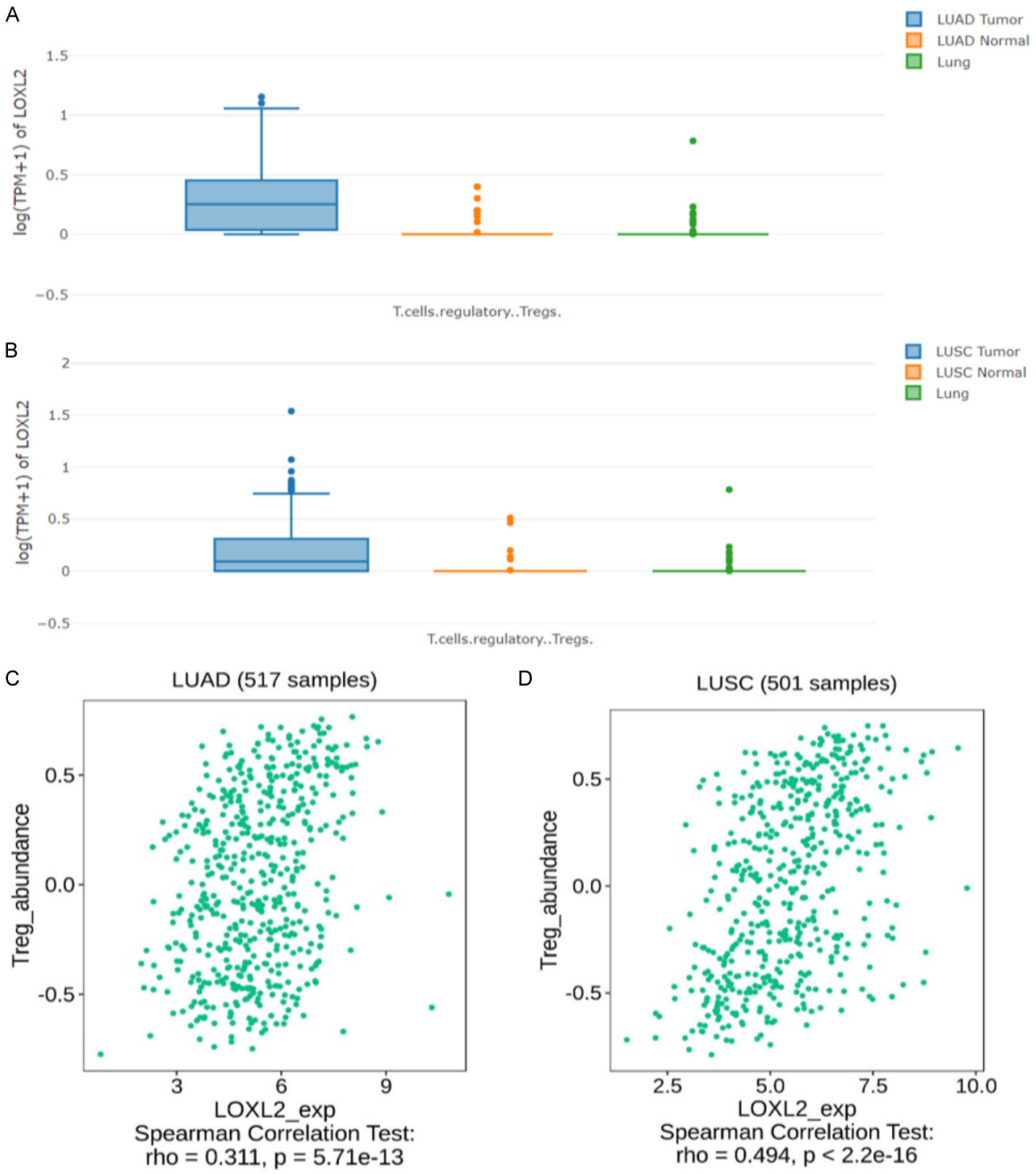

Figure 3. *LOXL2* was positively correlated with T-reg. A, B. Correlation between *LOXL2* expression and T-reg in LUAD and LUSC patients. C, D. Associations between *LOXL2* expression and immune subtypes in LUAD and LUSC.

LOXL2, LOXL3, and LOXL4, has been demonstrated to enhance extracellular matrix stability by cross-linking elastin and collagen in the outer matrix [23, 24]. Recent studies have demonstrated that LOX also facilitates tumor cell migration and invasion through a number of mechanisms, including the promotion of epithelial-mesenchymal transition (EMT) [25], the activation of the p-FAK/p-paxillin/YAP signaling pathway [26] and the involvement in the formation of a pre-metastatic microenvironment [27]. This has been demonstrated to be a crucial factor in the process of tumorigenesis and metastasis [26, 28]. It is anticipated that this will prove to be a promising target for tumor therapy. Among these, lysyl oxidase-like 2 (*LOXL2*) has been identified as a gene that upregulation promotes tumor infiltration and metastasis

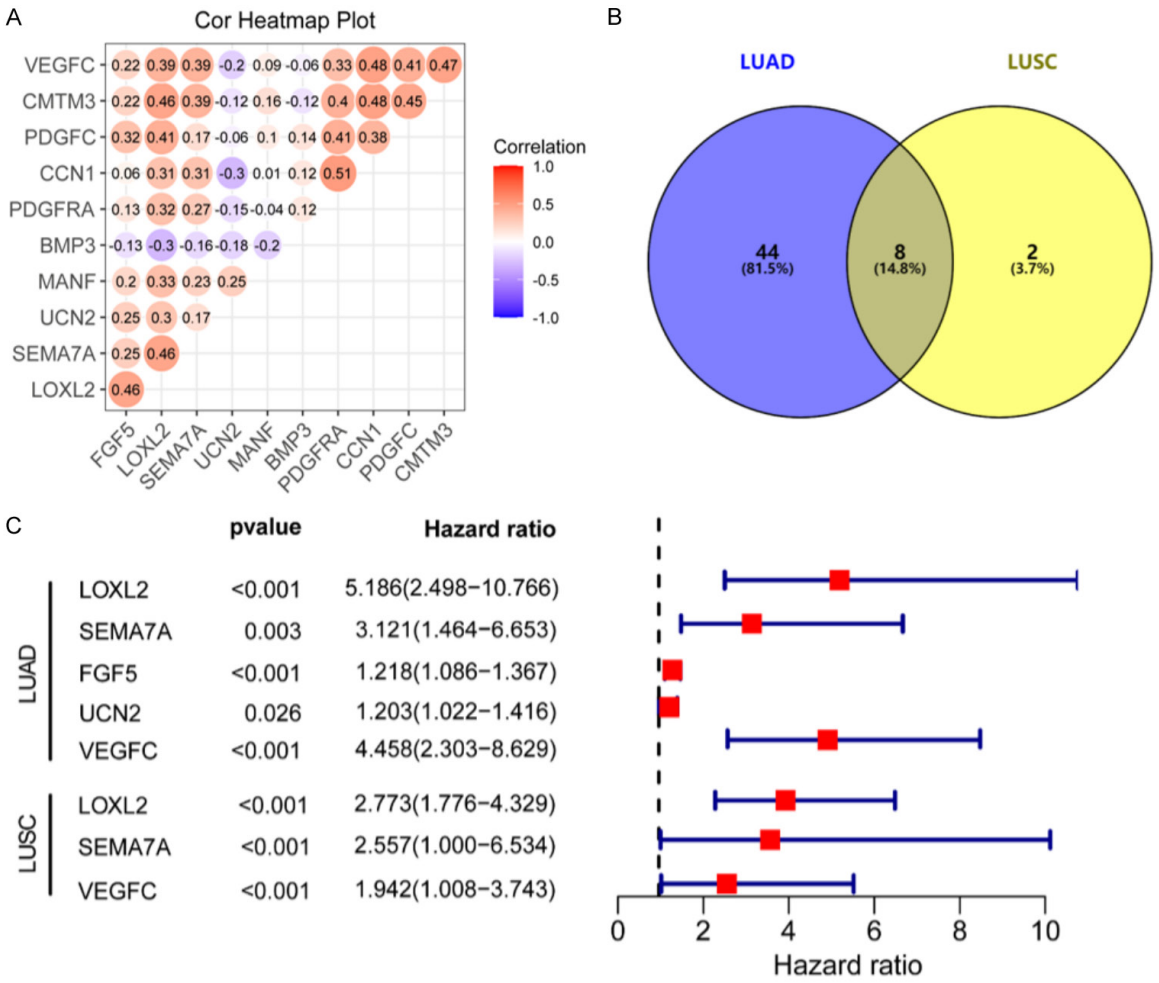

Figure 4. *SEMA7A* and *VEGFC* positively correlate with *LOXL2* in non-small cell lung cancer. A. Correlation analysis of the differential up-regulation and down-regulation of related genes on LUAD and LUSC. B. Venn diagrams of genes related to *LOXL2* in LUAD and LUSC. C. The 2 intersection genes that related to OS were extracted by univariate Cox regression analysis.

[29]. The aberrant expression of *LOXL2* in various tumors has been associated with several adverse outcomes, including epithelial-mesenchymal transition (EMT), metastasis, poor prognosis, chemo-radiotherapy resistance, and tumor progression [29, 30]. Previous study demonstrated that *LOX* and *LOXL2* are directly regulated by the miR-00/ZEB1 axis, and that *LOXL2* might serve as a new target for lung cancer therapy [31]. Subsequently, a number of studies demonstrated a correlation between elevated LOXL2 expression and reduced overall survival, as well as worsening of clinicopathological features of tumors [32]. Furthermore, our findings indicate that LOXL2 is highly expressed in non-small cell lung cancer and is associated with a poor prognosis. Consequently, it is postulated that LOXL2 may represent a novel therapeutic target for the treatment of NSCLC.

Consequently, we calculated the immune, matrix, and tumor purity of LUAD and LUSC and confirmed that LOXL2 was associated with the immune response of NSCLC. The relationship between LOXL2 and T-reg was identified through the analysis of the degree of immune infiltration and the proportion of immune T cells. A positive correlation was observed between LOXL2 and T-reg. Moreover, regulatory T cells (Tregs) have been shown to promote immune suppression in malignant tumors by suppressing the immune response to cancer cells [33]. Treg cells plays a pivotal role in main-

Table 3. Association of fifty-two corresponding bases of LUAD with LOXL2

GENE1	GENE2	P	R
LOXL2	PDGFRA	2.97444E-20	0.36848778
LOXL2	GDF11	2.49057E-14	0.308106677
LOXL2	SEMA4F	2.31871E-18	0.350596022
LOXL2	IL1RN	4.10483E-17	0.385049349
LOXL2	CCL21	9.49702E-19	0.35435584
LOXL2	SEMA7A	2.8837E-58	0.599078545
LOXL2	FGF5	3.26866E-26	0.418530278
LOXL2	CMTM3	8.7196E-62	0.613532508
LOXL2	SECTM1	2.27652E-15	0.319714484
LOXL2	HDGF	3.45809E-45	0.537939759
LOXL2	GDF7	1.51068E-17	-0.342533156
LOXL2	UCN2	1.5078E-16	0.371179367
LOXL2	MANF	2.4182E-42	0.522782038
LOXL2	PDGFC	1.18991E-18	0.398061079
LOXL2	ADM	3.65267E-40	0.510629978
LOXL2	VEGFC	3.21155E-45	0.538106606
LOXL2	STC1	2.41538E-69	0.659673055
LOXL2	GIP	6.12859E-12	0.336351246
LOXL2	TOR2A	3.65868E-16	0.32825584
LOXL2	TGFA	5.19121E-15	0.366262391
LOXL2	AIMP1	1.3148E-23	0.397702146
LOXL2	ESM1	1.50638E-46	0.569273722
LOXL2	GREM1	4.3189E-51	0.567128278
LOXL2	SEMA6B	1.78133E-43	0.554551206
LOXL2	CD320	8.90038E-25	0.407236163
LOXL2	LTBP3	1.33309E-16	0.332859725
LOXL2	BMP1	2.52567E-83	0.688311411
LOXL2	SEMA4C	5.06991E-51	0.566800334
LOXL2	CXCL8	7.83508E-26	0.452239551
LOXL2	APLN	4.08522E-20	0.367221915
LOXL2	ANGPTL7	3.20052E-15	-0.318092326
LOXL2	CCL11	3.29126E-16	0.328742125
LOXL2	SAA1	6.0212E-17	0.336430152
LOXL2	VEGFB	2.92379E-25	0.411089378
LOXL2	CLCF1	5.6556E-24	0.400722429
LOXL2	DEFB103B	1.09719E-15	0.323157274
LOXL2	RABEP2	9.27753E-14	0.301500619
LOXL2	BMP8A	4.29787E-12	0.337930853
LOXL2	CSF1	4.10798E-12	0.338131359
LOXL2	JAG2	5.90689E-31	0.453085117
LOXL2	SEMA4B	3.73141E-58	0.618957825
LOXL2	ANGPTL5	7.44501E-11	-0.324968647
LOXL2	SEMA4D	1.59881E-11	0.332036618
LOXL2	FAM3C	1.75315E-35	0.512438649
LOXL2	GMFB	2.65536E-18	0.350020547
LOXL2	NMB	8.22844E-11	0.324502476
LOXL2	S100A6	8.25088E-21	0.415408511
LOXL2	DEFA1	3.48669E-14	0.306432507
LOXL2	CKLF	1.41157E-25	0.413583014
LOXL2	MIF	2.19098E-20	0.412079957
LOXL2	CCL16	1.58955E-15	-0.321414289
LOXL2	CCL3	1.29679E-10	0.322372806

Table 4. Association of ten related genes of LUSC with LOXL2

GENE1	GENE2	P	R
LOXL2	PDGFRA	5.46926E-10	0.32491428
LOXL2	SEMA7A	7.77056E-30	0.457736861
LOXL2	FGF5	1.305E-30	463270539
LOXL2	CMTM3	4.11249E-30	45972208
LOXL2	CCN1	1.83492E-13	306935752
LOXL2	UCN2	4.35921E-13	0.302312857
LOXL2	MANF	1.4595E-11	0.331374895
LOXL2	PDGFC	1.75505E-23	0.408057926
LOXL2	VEGFC	7.30389E-17	0.393951854
LOXL2	BMP3	3.60237E-13	-0.303338747

taining peripheral tolerance in vivo through the active suppression of self-reactive T-cell activation and expansion. This helps to prevent autoimmune diseases and restrain chronic inflammatory conditions [34]. In patients with early-stage NSCLC, an increased number of circulating and tumor-infiltrating regulatory Tregs are associated with a poorer prognosis and a higher risk of recurrence [35]. In light of these findings, *LOXL2* may serve as a promising novel marker for the treatment of LUAD and LUSC, as well as for prognostication.

To further confirmed the prognostic indicative role of *LOXL2* in patients with non-small cell lung cancer, we searched for the related molecules of *LOXL2* and performed multi-factor Cox survival analysis to identify two prognostic factors *SMEATA* and *VEGFC. SEMA7A,* a glycosylphosphatidylinositol-anchored (GPI-anchored) glycoprotein on the plasma membrane. Recent research has shown that FUT8-mediated aberrant N-glycosylation of SEMA7A promotes head and neck squamous cell carcinoma progression [36]. It is a possible therapeutic target for patients with *EGFR-TKI*-resistant lung adenocarcinoma [37]. *VEGFC*, a member of the vascular endothelial growth factor/platelet-derived growth factor family, promotes endothelial cell proliferation and angiogenesis. VEGF family consists of seven members, including VEGF-A, VEGF-B, VEGF-C, VEGF-D, placental growth factor (PlGF), and non-human genome encoded VEGF-E and svVEGF [38]. VEGFC promotes tumor growth and metastasis through lymphangiogenesis and lymphatic metastasis, which is mediated by VEGFR-3 [39]. Blocking this pathway leads to apoptosis of lymphatic endothelial cells and disruption of the lymphatic network. Thus,

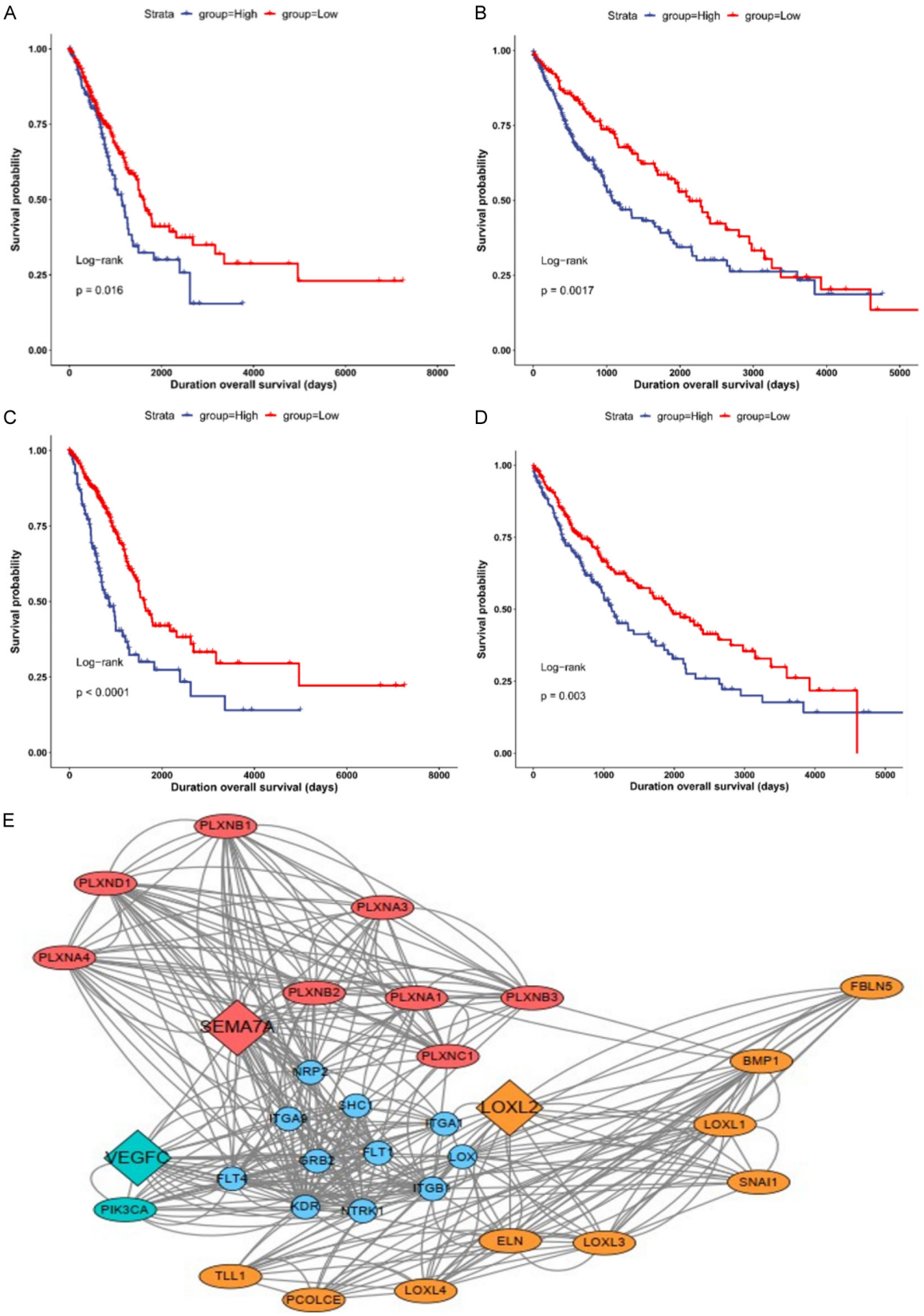

Figure 5. *SEMA7A* and *VEGFC* are prognostic factors in LUAD and LUSC. A, B. The Kaplan-Meier plot of SEMA7A in LUAD and LUSC. C, D. The Kaplan-Meier plot of *VEGFC* in LUAD and LUSC. E. Protein-protein interaction (PPI) network. Molecules with the highest correlation with *LOXL2*.

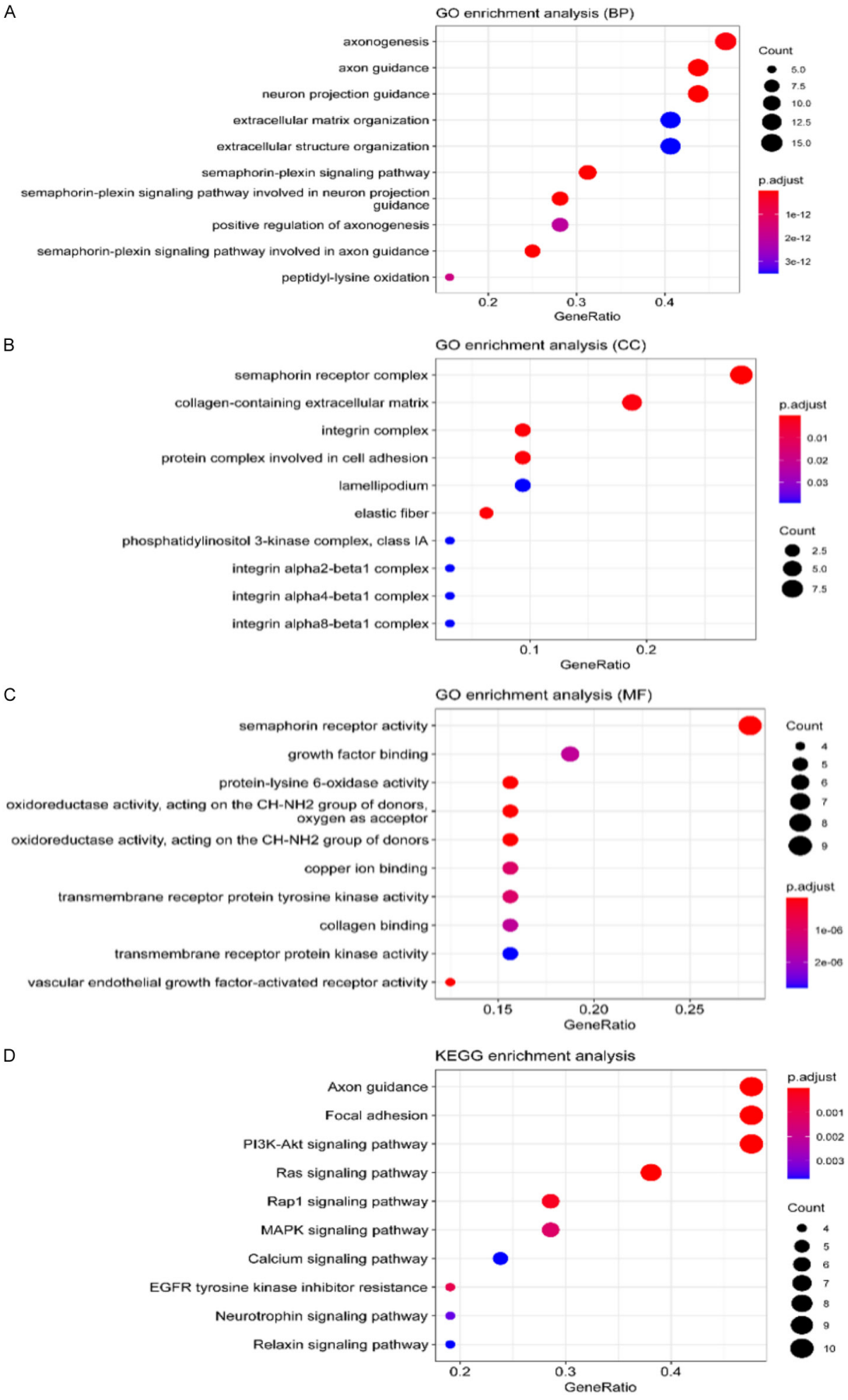
A
GO enrichment analysis (BP)
axonogenesis
axon guidance
neuron projection guidance
extracellular matrix organization
extracellular structure organization
semaphorin-plexin signaling pathway
semaphorin-plexin signaling pathway involved in neuron projection guidance
positive regulation of axonogenesis
semaphorin-plexin signaling pathway involved in axon guidance
peptidyl-lysine oxidation
0.2
0.3
0.4
GeneRatio
Count
5.0
7.5
10.0
12.5
15.0
p.adjust
1e-12
2e-12
3e-12
B
GO enrichment analysis (CC)
semaphorin receptor complex
collagen-containing extracellular matrix
integrin complex
protein complex involved in cell adhesion
lamellipodium
elastic fiber
phosphatidylinositol 3-kinase complex, class IA
integrin alpha2-beta1 complex
integrin alpha4-beta1 complex
integrin alpha8-beta1 complex
0.1
0.2
GeneRatio
p.adjust
0.01
0.02
0.03
Count
2.5
5.0
7.5
C
GO enrichment analysis (MF)
semaphorin receptor activity
growth factor binding
protein-lysine 6-oxidase activity
oxidoreductase activity, acting on the CH-NH2 group of donors, oxygen as acceptor
oxidoreductase activity, acting on the CH-NH2 group of donors
copper ion binding
transmembrane receptor protein tyrosine kinase activity
collagen binding
transmembrane receptor protein kinase activity
vascular endothelial growth factor-activated receptor activity
0.15
0.20
0.25
GeneRatio
Count
4
5
6
7
8
9
p.adjust
1e-06
2e-06
D
KEGG enrichment analysis
Axon guidance
Focal adhesion
PI3K-Akt signaling pathway
Ras signaling pathway
Rap1 signaling pathway
MAPK signaling pathway
Calcium signaling pathway
EGFR tyrosine kinase inhibitor resistance
Neurotrophin signaling pathway
Relaxin signaling pathway
0.2
0.3
0.4
GeneRatio
p.adjust
0.001
0.002
0.003
Count
4
5
6
7
8
9
10

Figure 6. The tasks of *LOXL2* and the correlations among their functions. A-D. Bar plot of Go and KEGG functional enrichment analyses. BP indicated biological process; CC indicated cellular component; MF indicated molecular function.

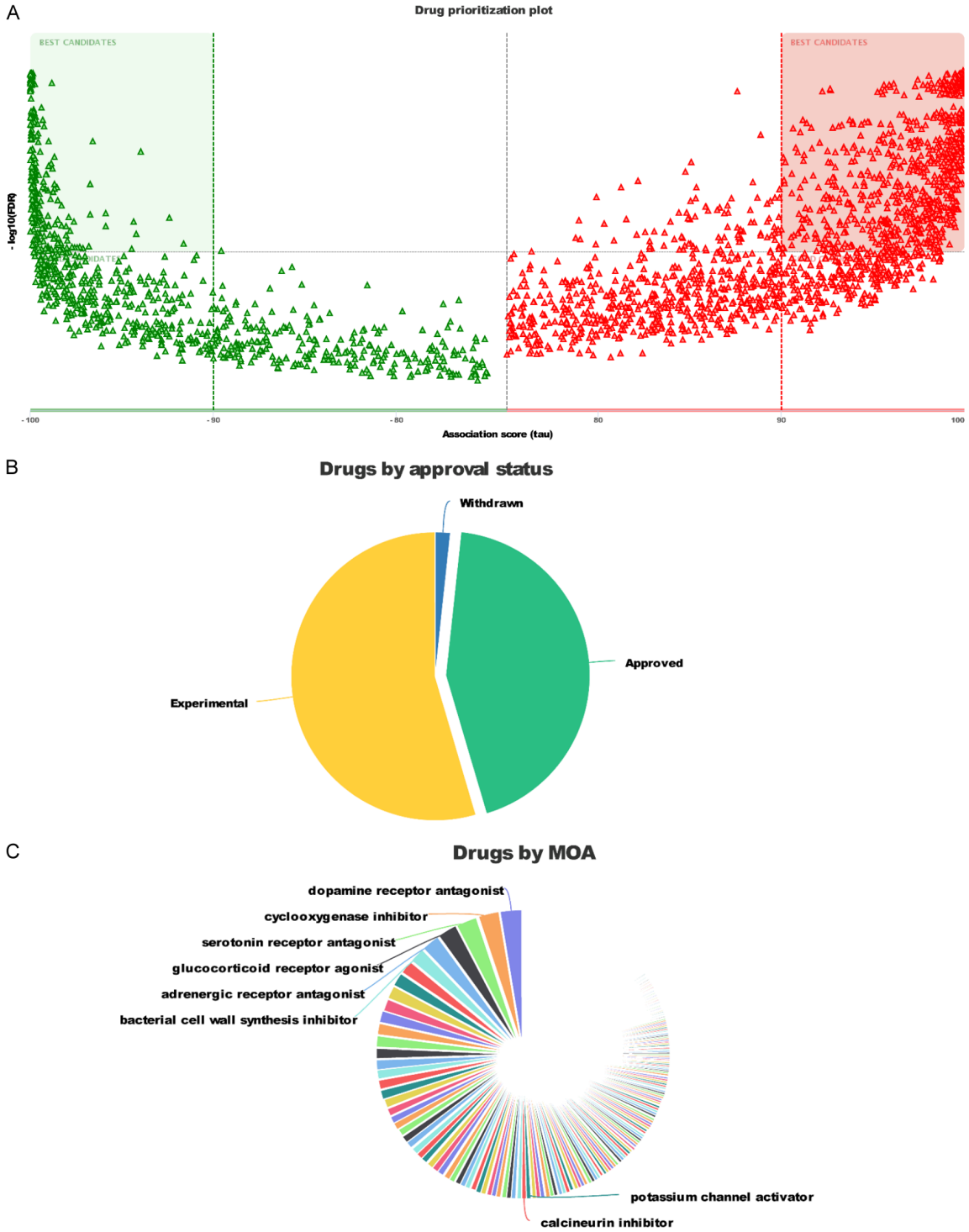

Figure 7. The therapeutic targets and mechanisms of drugs. A. Volcano plots shows the priorities of different medicines found in the DREIMT database. B. The mechanism of action of tumor drugs on the market. C. Classification of the medications for treating tumors according to their approval status.

Table 5. Common tumor treatment drugs on the market

Drug_name	Drug_pubchm_id	Summary	FDR	tau	Drug specificity_score	Drug_source_db	Drug_source_name	Drug_status	Drug_moa	Drug_target_gene_names	Drug_target_gene_ids
Cefuroxime	5361202	Cefuroxime boosts case type compared to reference type	0.001652893	99.98135372		LINCS	BRD-K63641886	APPROVED	Bacterial cell wall synthesis inhibitor		
Calcifediol		Calcifediol boosts case type compared to reference type	0.001788909	99.98135372	0.55427037	LINCS	BRD-K77175907	APPROVED	Vitamin D receptor agonist	VDR	7421
Benzocaine	2337	Benzocaine boosts case type compared to reference type	0.001841621	99.98135372		LINCS	BRD-K75466013	APPROVED	Sodium channel blocker	SCN10A	6336
Cefazolin		Cefazolin boosts case type compared to reference type	0.001851852	99.98135372		LINCS		APPROVED	Bacterial cell wall synthesis inhibitor	PON1	5444
Mesoridazine	4078	Mesoridazine boosts case type compared to reference type	0.001901141	99.98135372	0.6460514	LINCS	BRD-A14395271	APPROVED	Dopamine receptor antagonist	HTR2A, DRD2	3356, 1813
Tacrolimus	445643	Tacrolimus boosts case type compared to reference type	0.002028398	99.98135372	0.61548928	LINCS	BRD-K65261396	APPROVED	Calcineurin inhibitor	FKBP1A	2280
Rimantadine	5071	Rimantadine boosts case type compared to reference type	0.002325581	99.98135372		LINCS		APPROVED	Antiviral, RNA synthesis inhibitor		
Doxorubicin	31703	Doxorubicin boosts case type compared to reference type	0.002421308	99.98135372	0.69624245	LINCS	BRD-A52530684	APPROVED	Topoisomerase inhibitor	TOP2A	7153
Cefuroxime	5361202	Cefuroxime boosts case type compared to reference type	0.001623377	99.96270744		LINCS		APPROVED	Bacterial cell wall synthesis inhibitor		
Guanethidine	3518	Guanethidine boosts case type compared to reference type	0.001766784	99.96270744		LINCS	BRD-M18219129	APPROVED	Adrenergic inhibitor	SLC6A2	6530

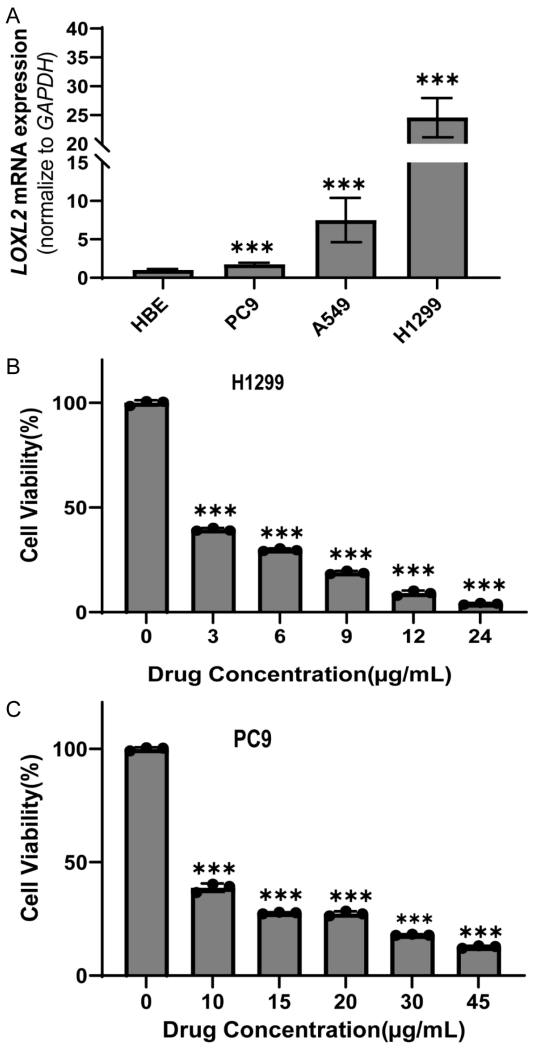

Figure 8. Drug sensitivity experiments of doxorubicin on *LOXL2* expression profile. A. The expression of *LOXL2 mRNA* in NSCLC assessed using RT-qPCR (n=12, ***P<0.001). B, C. Cell Counting Kit-8 assay was employed to ascertain the half maximal inhibitory concentration (IC_{50}) of doxorubicin at varying concentration gradients on the H1299 cell line, exhibiting robust *LOXL2* expression and PC9 cell line, characterized by relatively low *LOXL2* expression (n=3, ***P<0.001).

VEGFC is involved in lymphatic metastasis of tumor, which is a feature of poor tumor prognosis [40, 41]. These two prognostic factors are further evidence for the prognostic role of LOXL2 in NSCLC.

The "oncoPredict" is an R package for predicting drug responses. It integrates three approaches to (1) correct for overall drug sensitivity for drug-specific biomarker discovery, (2) predict a patient's clinical drug response, and (3) correlate these predictions with clinical features for in vivo drug biomarker discovery. This new "oncoPredict" R software package can be applied to a variety of in vitro and in vivo drug and biomarker discovery settings [42]. We use the "oncoPredict" R package to analyze the batch-corrected prioritization of different drugs in the DREAMT database. Nine drugs are tested: cefuroxime benzocaine, benzocaine, cefazolin, methotrexate, tacrolimus, rimantadine, doxorubicin, cefuroxime and guanethidine. In order to investigate the relationship between *LOXL2* expression and drug sensitivity, we proceeded to identify the compounds with the strongest correlation with *LOXL2* levels, which were then subjected to subsequent experiments. The results demonstrated that the H1299 cell line, which exhibited higher *LOXL2* expression, exhibited greater sensitivity to doxorubicin compared to the PC9 cell line, which exhibited lower *LOXL2* expression. These findings illustrate the potential role of *LOXL2* in predicting drug response and emphasize the importance of considering gene expression levels when selecting compounds for therapeutic intervention.

This study has some limitations. Our study is a retrospective, not a prospective analysis, and we analyze the role of LOXL2 in NSCLC by bioinformatics analysis without exploring the mechanism. In conclusion, our results indicate a prognostic role of *LOXL2* in NSCLC patients. The analysis of the tumor immune microenvironment suggests the possibility of *LOXL2* as a new target for immunotherapy of NSCLC. The results of molecular interactions reveal that *SEMA7A* and *VEGFC* may be prognostic factors in NSCLC.

Acknowledgements

This study was supported by research grants from the National Natural Science Foundation of China under grant 82171576, and Jiangsu Province Capability Improvement Project through Science, Technology and Education under grant No. CXZX202228 to Jianqing Wu.

Disclosure of conflict of interest

None.

Address correspondence to: Jianqing Wu, Department of Geriatrics, Key Laboratory of Geriatrics of

Jiangsu Province, The First Affiliated Hospital of Nanjing Medical University, 300 Guangzhou Road, Nanjing 210029, Jiangsu, China. Tel: +86-25-83563026; Fax: +86-25-83780170; E-mail: jwuny@njmu.edu.cn

References

[1] Leiter A, Veluswamy RR and Wisnivesky JP. The global burden of lung cancer: current status and future trends. Nat Rev Clin Oncol 2023; 20: 624-639.

[2] Qi J, Li M, Wang L, Hu Y, Liu W, Long Z, Zhou Z, Yin P and Zhou M. National and subnational trends in cancer burden in China, 2005-20: an analysis of national mortality surveillance data. Lancet Public Health 2023; 8: e943-e955.

[3] Lancaster HL, Heuvelmans MA and Oudkerk M. Low-dose computed tomography lung cancer screening: clinical evidence and implementation research. J Intern Med 2022; 292: 68-80.

[4] Hanna NH, Schneider BJ, Temin S, Baker S Jr, Brahmer J, Ellis PM, Gaspar LE, Haddad RY, Hesketh PJ, Jain D, Jaiyesimi I, Johnson DH, Leighl NB, Phillips T, Riely GJ, Robinson AG, Rosell R, Schiller JH, Singh N, Spigel DR, Stabler JO, Tashbar J and Masters G. Therapy for Stage IV non-small-cell lung cancer without driver alterations: ASCO and OH (CCO) joint guideline update. J Clin Oncol 2020; 38: 1608-1632.

[5] Al Bakir M, Huebner A, Martinez-Ruiz C, Grigoriadis K, Watkins TBK, Pich O, Moore DA, Veeriah S, Ward S, Laycock J, Johnson D, Rowan A, Razaq M, Akther M, Naceur-Lombardelli C, Prymas P, Toncheva A, Hessey S, Dietzen M, Colliver E, Frankell AM, Bunkum A, Lim EL, Karasaki T, Abbosh C, Hiley CT, Hill MS, Cook DE, Wilson GA, Salgado R, Nye E, Stone RK, Fennell DA, Price G, Kerr KM, Naidu B, Middleton G, Summers Y, Lindsay CR, Blackhall FH, Cave J, Blyth KG, Nair A, Ahmed A, Taylor MN, Procter AJ, Falzon M, Lawrence D, Navani N, Thakrar RM, Janes SM, Papadatos-Pastos D, Forster MD, Lee SM, Ahmad T, Quezada SA, Peggs KS, Van Loo P, Dive C, Hackshaw A, Birkbak NJ, Zaccaria S; RACERx Consortium, Jamal-Hanjani M, McGranahan N and Swanton C. The evolution of non-small cell lung cancer metastases in TRACERx. Nature 2023; 616: 534-542.

[6] Hynds RE, Huebner A, Pearce DR, Hill MS, Akarca AU, Moore DA, Ward S, Gowers KHC, Karasaki T, Al Bakir M, Wilson GA, Pich O, Martinez-Ruiz C, Hossain ASMM, Pearce SP, Sivakumar M, Ben Aissa A, Gronroos E, Chandrasekharan D, Kolluri KK, Towns R, Wang K, Cook DE, Bosshard-Carter L, Naceur-Lombardelli C, Rowan AJ, Veeriah S, Litchfield K, Crosbie PAJ, Dive C, Quezada SA, Janes SM, Jamal-Hanjani M, Marafioti T; TRACERx Consortium, McGranahan N and Swanton C. Representation of genomic intratumor heterogeneity in multi-region non-small cell lung cancer patient-derived xenograft models. Nat Commun 2024; 15: 4653.

[7] Wang C, Yu Q, Song T, Wang Z, Song L, Yang Y, Shao J, Li J, Ni Y, Chao N, Zhang L and Li W. The heterogeneous immune landscape between lung adenocarcinoma and squamous carcinoma revealed by single-cell RNA sequencing. Signal Transduct Target Ther 2022; 7: 289.

[8] Wang W, Zhao M, Cui L, Ren Y, Zhang J, Chen J, Jia L, Zhang J, Yang J, Chen G, Ashby CR Jr, Wu C, Chen ZS and Wang L. Characterization of a novel HDAC/RXR/HtrA1 signaling axis as a novel target to overcome cisplatin resistance in human non-small cell lung cancer. Mol Cancer 2020; 19: 134.

[9] Allaeys T, Berzenji L, Lauwers P, Yogeswaran SK, Hendriks JMH, Billiet C, De Bondt C and Van Schil PE. Multimodality treatment including surgery related to the type of N2 involvement in locally advanced non-small cell lung cancer. Cancers (Basel) 2022; 14: 1656.

[10] Zhou H, Zhou L, Guan Q, Hou X, Wang C, Liu L, Wang J, Yu X, Li W and Liu H. Skp2-mediated MLKL degradation confers cisplatin-resistant in non-small cell lung cancer cells. Commun Biol 2023; 6: 805.

[11] Li Y, Yang X, Sun Y, Li Z, Yang W, Ju B, Easton J, Pei D, Cheng C, Lee S, Pui CH, Yu J, Chi H and Yang JJ. Impact of T-cell immunity on chemotherapy response in childhood acute lymphoblastic leukemia. Blood 2022; 140: 1507-1521.

[12] Bhardwaj N. Harnessing the immune system to treat cancer. J Clin Invest 2007; 117: 1130-1136.

[13] Lahiri A, Maji A, Potdar PD, Singh N, Parikh P, Bisht B, Mukherjee A and Paul MK. Lung cancer immunotherapy: progress, pitfalls, and promises. Mol Cancer 2023; 22: 40.

[14] Kennedy LB and Salama AKS. A review of cancer immunotherapy toxicity. CA Cancer J Clin 2020; 70: 86-104.

[15] Chow A, Perica K, Klebanoff CA and Wolchok JD. Clinical implications of T cell exhaustion for cancer immunotherapy. Nat Rev Clin Oncol 2022; 19: 775-790.

[16] Zhou F, Qiao M and Zhou C. The cutting-edge progress of immune-checkpoint blockade in lung cancer. Cell Mol Immunol 2021; 18: 279-293.

[17] Giannone G, Ghisoni E, Genta S, Scotto G, Tuninetti V, Turinetto M and Valabrega G.

Immuno-metabolism and microenvironment in cancer: key players for immunotherapy. Int J Mol Sci 2020; 21: 4414.
[18] Fan L, Jiang W, Chen C, Gao H, Shi J and Wang D. CEBPA facilitates LOXL2 and LOXL3 transcription to promote BCL-2 stability and thus enhances the growth and metastasis of lung carcinoma cells in vitro. Exp Cell Res 2024; 435: 113937.
[19] Su CC, Wu JT, Choi E, Myall NJ, Neal JW, Kurian AW, Stehr H, Wood D, Henry SM, Backhus LM, Leung AN, Wakelee HA and Han SS. Overall survival among patients with de novo stage iv metastatic and distant metastatic recurrent non-small cell lung cancer. JAMA Netw Open 2023; 6: e2335813.
[20] Liu Z, Shi M, Ren Y, Xu H, Weng S, Ning W, Ge X, Liu L, Guo C, Duo M, Li L, Li J and Han X. Recent advances and applications of CRISPR-Cas9 in cancer immunotherapy. Mol Cancer 2023; 22: 35.
[21] Larson RC and Maus MV. Recent advances and discoveries in the mechanisms and functions of CAR T cells. Nat Rev Cancer 2021; 21: 145-161.
[22] Oliveira G and Wu CJ. Dynamics and specificities of T cells in cancer immunotherapy. Nat Rev Cancer 2023; 23: 295-316.
[23] Zheng C, Chu Y, Zhang N, Jia T, Li Y, Jiang T and Sun J. Pan-cancer analysis of the LOx family reveals that LOX affects tumor prognosis by affecting immune infiltration. Crit Rev Eukaryot Gene Expr 2024; 34: 87-100.
[24] Liburkin-Dan T, Toledano S and Neufeld G. Lysyl oxidase family enzymes and their role in tumor progression. Int J Mol Sci 2022; 23: 6249.
[25] Alonso-Nocelo M, Ruiz-Canas L, Sancho P, Gorgulu K, Alcala S, Pedrero C, Vallespinos M, Lopez-Gil JC, Ochando M, Garcia-Garcia E, David Trabulo SM, Martinelli P, Sanchez-Tomero P, Sanchez-Palomo C, Gonzalez-Santamaria P, Yuste L, Wormann SM, Kabacaoglu D, Earl J, Martin A, Salvador F, Valle S, Martin-Hijano L, Carrato A, Erkan M, Garcia-Bermejo L, Hermann PC, Algul H, Moreno-Bueno G, Heeschen C, Portillo F, Cano A and Sainz B Jr. Macrophages direct cancer cells through a LOXL2-mediated metastatic cascade in pancreatic ductal adenocarcinoma. Gut 2023; 72: 345-359.
[26] Liu X, Li J, Yang X, Li X, Kong J, Qi D, Zhang F, Sun B, Liu Y and Liu T. Carcinoma-associated fibroblast-derived lysyl oxidase-rich extracellular vesicles mediate collagen crosslinking and promote epithelial-mesenchymal transition via p-FAK/p-paxillin/YAP signaling. Int J Oral Sci 2023; 15: 32.
[27] Urooj T, Wasim B, Mushtaq S, Shah SNN and Shah M. Cancer cell-derived secretory factors in breast cancer-associated lung metastasis: their mechanism and future prospects. Curr Cancer Drug Targets 2020; 20: 168-186.
[28] Umezaki N, Nakagawa S, Yamashita YI, Kitano Y, Arima K, Miyata T, Hiyoshi Y, Okabe H, Nitta H, Hayashi H, Imai K, Chikamoto A and Baba H. Lysyl oxidase induces epithelial-mesenchymal transition and predicts intrahepatic metastasis of hepatocellular carcinoma. Cancer Sci 2019; 110: 2033-2043.
[29] Cano A, Eraso P, Mazon MJ and Portillo F. LOXL2 in cancer: a two-decade perspective. Int J Mol Sci 2023; 24: 14405.
[30] Chitty JL, Yam M, Perryman L, Parker AL, Skhinas JN, Setargew YFI, Mok ETY, Tran E, Grant RD, Latham SL, Pereira BA, Ritchie SC, Murphy KJ, Trpceski M, Findlay AD, Melenec P, Filipe EC, Nadalini A, Velayuthar S, Major G, Wyllie K, Papanicolaou M, Ratnaseelan S, Phillips PA, Sharbeen G, Youkhana J, Russo A, Blackwell A, Hastings JF, Lucas MC, Chambers CR, Reed DA, Stoehr J, Vennin C, Pidsley R, Zaratzian A, Da Silva AM, Tayao M, Charlton B, Herrmann D, Nobis M, Clark SJ, Biankin AV, Johns AL, Croucher DR, Nagrial A, Gill AJ, Grimmond SM; Australian Pancreatic Cancer Genome Initiative (APGI); Australian Pancreatic Cancer Matrix Atlas (APMA), Pajic M, Timpson P, Jarolimek W and Cox TR. A first-in-class pan-lysyl oxidase inhibitor impairs stromal remodeling and enhances gemcitabine response and survival in pancreatic cancer. Nat Cancer 2023; 4: 1326-1344.
[31] Peng DH, Ungewiss C, Tong P, Byers LA, Wang J, Canales JR, Villalobos PA, Uraoka N, Mino B, Behrens C, Wistuba II, Han RI, Wanna CA, Fahrenholtz M, Grande-Allen KJ, Creighton CJ and Gibbons DL. ZEB1 induces LOXL2-mediated collagen stabilization and deposition in the extracellular matrix to drive lung cancer invasion and metastasis. Oncogene 2017; 36: 1925-1938.
[32] Deshpande H. Levoleucovorin inhibits LOXL2 (lysyl oxidase like-2) to control breast cancer proliferation: a repurposing approach. J Biomol Struct Dyn 2024; 42: 5104-5113.
[33] Dwivedi M, Tiwari S, Kemp EH and Begum R. Implications of regulatory T cells in anti-cancer immunity: from pathogenesis to therapeutics. Heliyon 2022; 8: e10450.
[34] Schloder J, Shahneh F, Schneider FJ and Wieschendorf B. Boosting regulatory T cell function for the treatment of autoimmune diseases - That's only half the battle! Front Immunol 2022; 13: 973813.
[35] Principe DR, Chiec L, Mohindra NA and Munshi HG. Regulatory T-cells as an emerging barrier to immune checkpoint inhibition in lung cancer. Front Oncol 2021; 11: 684098.

[36] Liu Z, Meng X, Zhang Y, Sun J, Tang X, Zhang Z, Liu L and He Y. FUT8-mediated aberrant N-glycosylation of SEMA7A promotes head and neck squamous cell carcinoma progression. Int J Oral Sci 2024; 16: 26.
[37] Passaro A, Janne PA, Mok T and Peters S. Overcoming therapy resistance in EGFR-mutant lung cancer. Nat Cancer 2021; 2: 377-391.
[38] Dakowicz D, Zajkowska M and Mroczko B. Relationship between VEGF family members, their receptors and cell death in the neoplastic transformation of colorectal cancer. Int J Mol Sci 2022; 23: 3375.
[39] Zheng H, Chen C, Luo Y, Yu M, He W, An M, Gao B, Kong Y, Ya Y, Lin Y, Li Y, Xie K, Huang J and Lin T. Tumor-derived exosomal BCYRN1 activates WNT5A/VEGF-C/VEGFR3 feedforward loop to drive lymphatic metastasis of bladder cancer. Clin Transl Med 2021; 11: e497.
[40] Pan Y, Liu L, Cheng Y, Yu J and Feng Y. Amplified LncRNA PVT1 promotes lung cancer proliferation and metastasis by facilitating VEGFC expression. Biochem Cell Biol 2020; 98: 676-682.
[41] Liu ZL, Chen HH, Zheng LL, Sun LP and Shi L. Angiogenic signaling pathways and anti-angiogenic therapy for cancer. Signal Transduct Target Ther 2023; 8: 198.
[42] Maeser D, Gruener RF and Huang RS. oncoPredict: an R package for predicting in vivo or cancer patient drug response and biomarkers from cell line screening data. Brief Bioinform 2021; 22: bbab260.

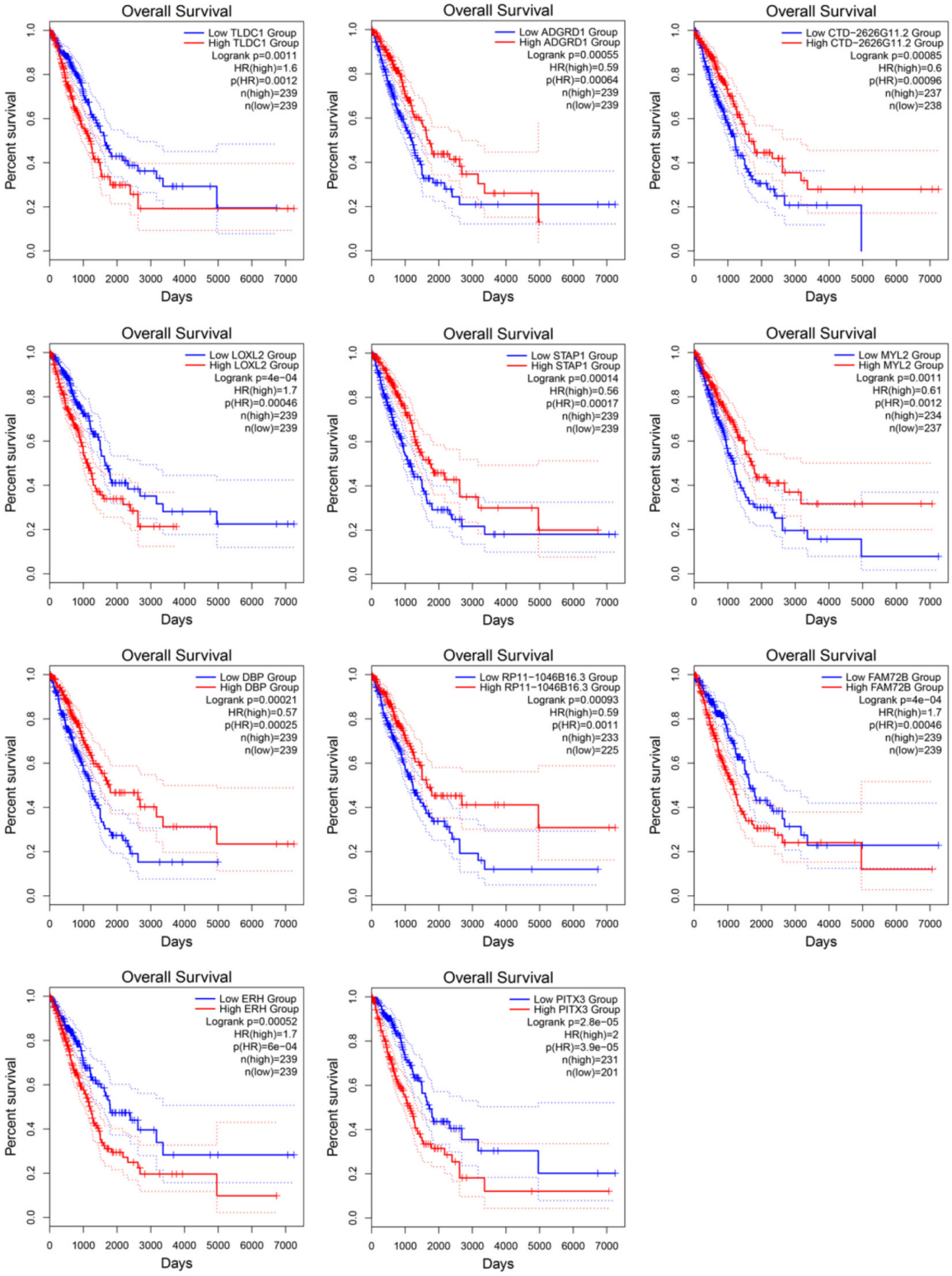

Figure S1. Survival curves of overall survival in LUAD in GEPIA cohorts.

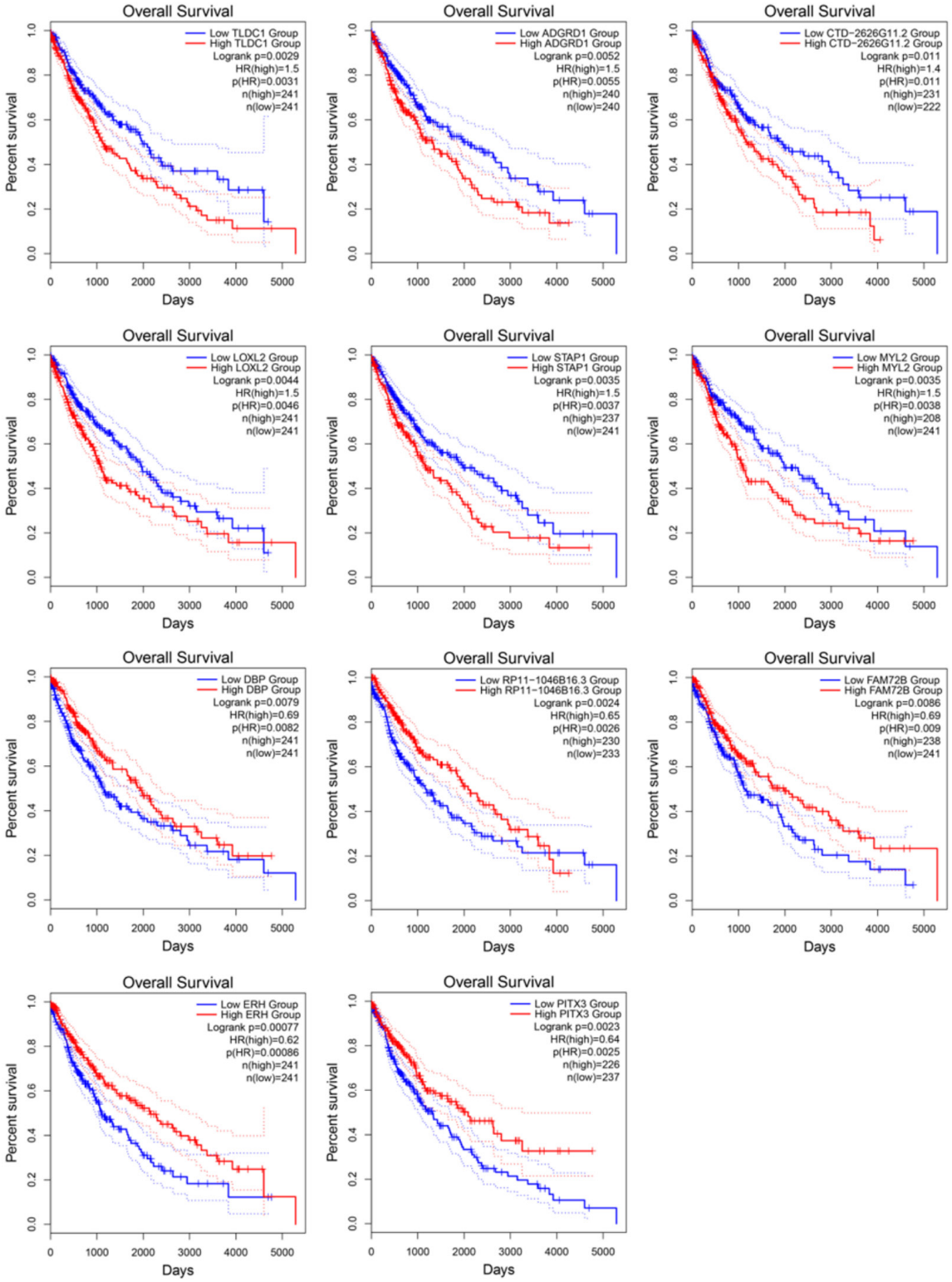

Figure S2. Survival curves of overall survival in LUSC in GEPIA cohorts.

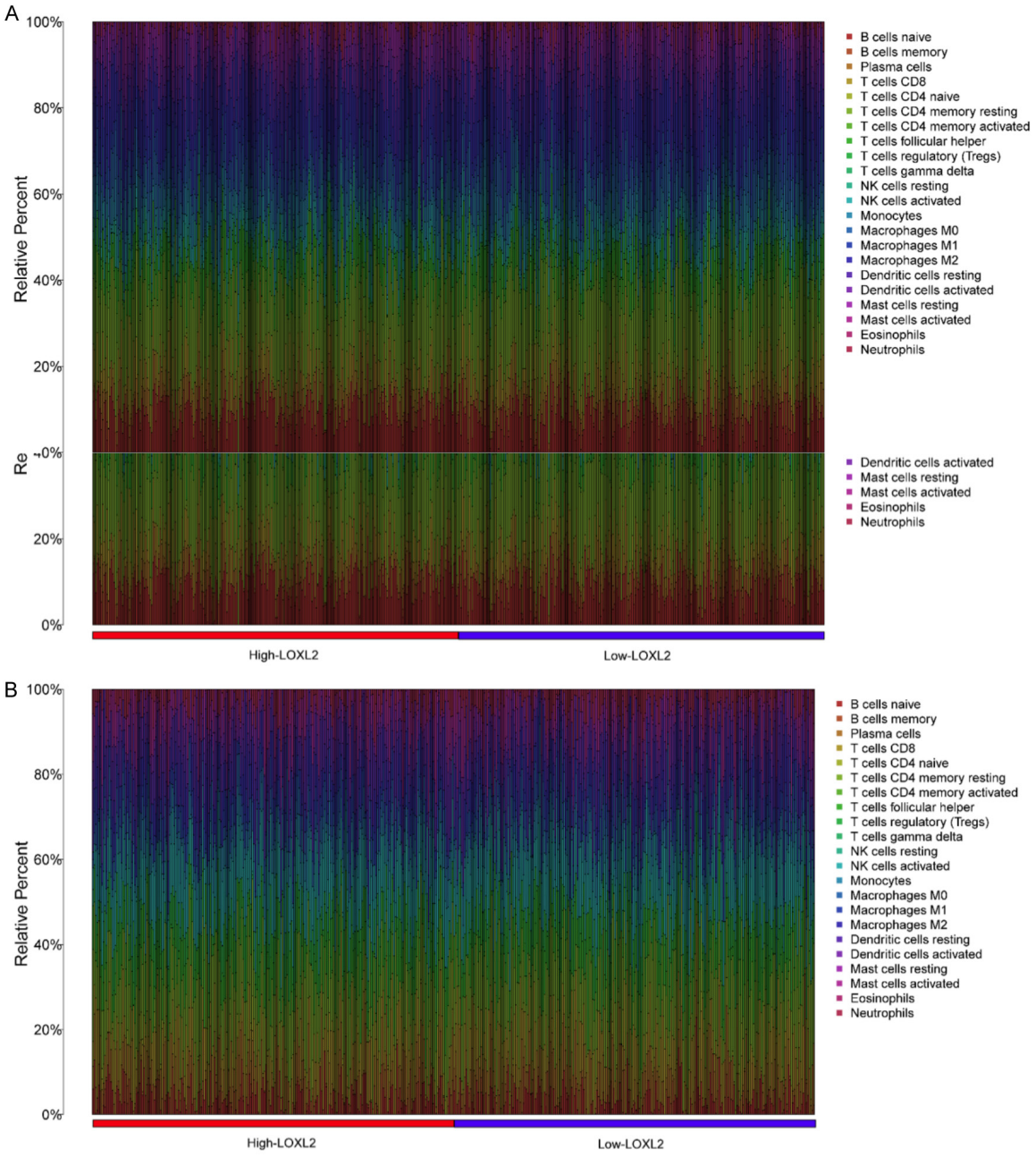

Figure S3. A, B. Taking the median TMB value as a cutoff, the relative expression of 22 tumor-infiltrating immune cells (Dendritic cells activated, Dendritic cells quiescent, Macrophages M2, T cell follicular helper cells, T cell regulatory (Tregs), T cell γδ, NK cells quiescent, NK cells activated, Monocytes, Macrophages M0, Macrophages M1, T cell CD4 memory activated, T cell CD4 memory quiescent, T cell CD4 naive, T cell CD8, Plasma cells, B cell memory, and B cell naive) in the low-TBM and high-TMB samples was determined.

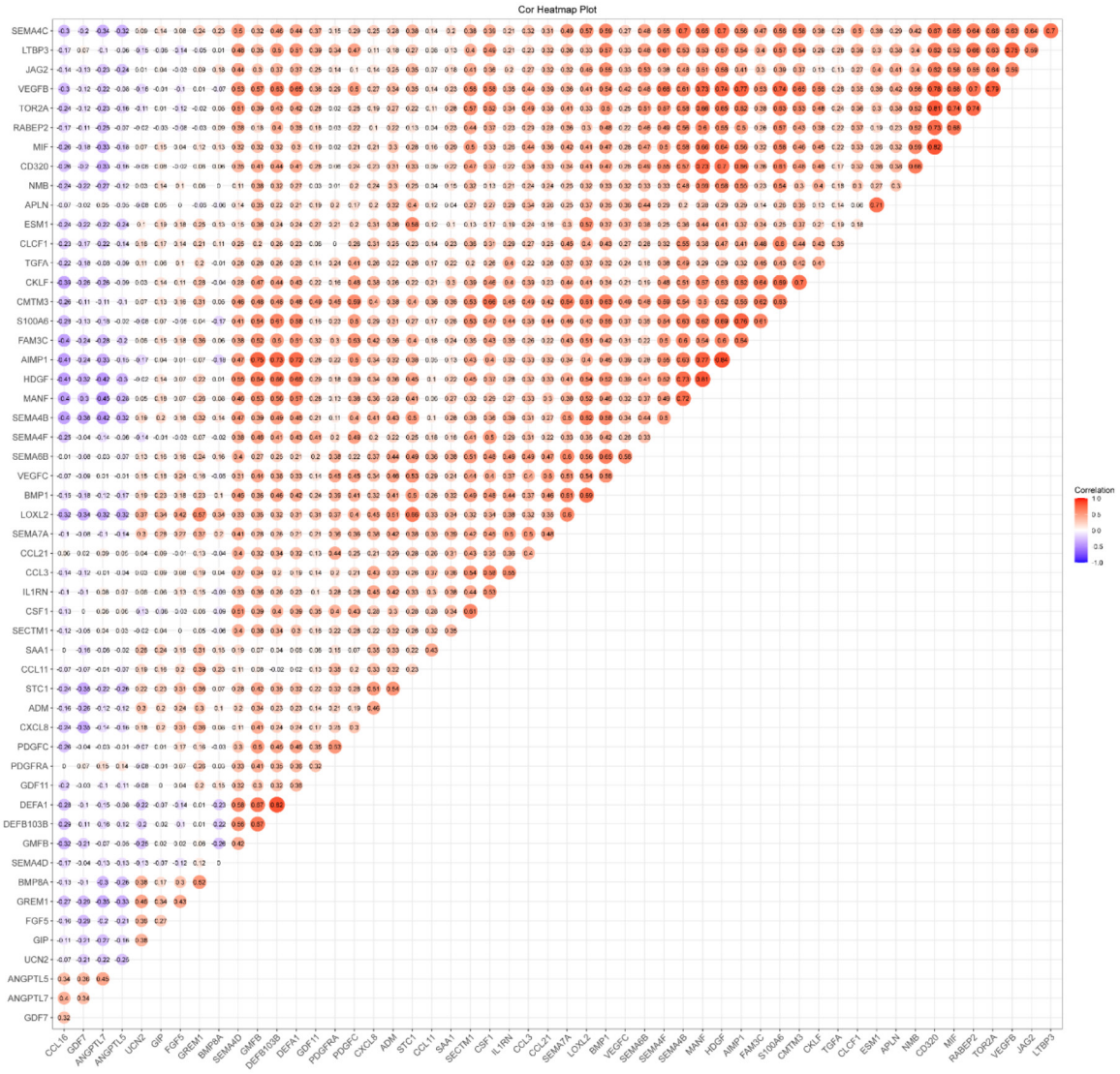

Figure S4. Correlation analysis of the differential up-regulation and down-regulation of related genes on LUAD and LUSC.